J Biol Inorg Chem (2001) 6 : 14–22
DOI 10.1007/s007750000177

ORIGINAL ARTICLE

**Catherine Hemmert · Marguerite Pitié
Michael Renz · Heinz Gornitzka · Stéphanie Soulet
Bernard Meunier**

Preparation, characterization and crystal structures of manganese(II), iron(III) and copper(II) complexes of the bis[di-1,1-(2-pyridyl)ethyl] amine (BDPEA) ligand; evaluation of their DNA cleavage activities

Received: 15 March 2000 / Accepted: 15 September 2000 / Published online: 28 November 2000

Abstract The synthesis of a new tetrapyridyl ligand, bis[di-1,1-(2-pyridyl)ethyl]amine (BDPEA), is described. Complexation of this ligand with manganese(II), iron(III) or copper(II) chlorides afforded mononuclear complexes: $Mn(BDPEA)Cl_2$ (**1**) $[Fe(BDPEA)Cl_2]Cl$ (**2**) and [Cu(BDPEA)Cl]Cl (**3**). In all cases, BDPEA is coordinated to the metal center by three pyridine nitrogen atoms and the secondary amine. The geometrical environments around the metals in $Mn(BDPEA)Cl_2$ and $[Fe(BDPEA)Cl_2]Cl$ are best described as distorted octahedrals and in [Cu(BDPEA)Cl]Cl as a slightly distorted square pyramid. The DNA cleavage activities of manganese(II), iron(III) or copper(II) complexes of both BDPEA and another tetrapyridyl ligand, bis[di(2-pyridyl)methyl]amine (BDPMA), in the presence of an oxidant (H_2O_2) or a reducing agent (ascorbate) with air, are reported. The iron(III) complexes exhibited significantly enhanced efficiencies, compared to copper(II) complexes. $[Fe(BDPEA)Cl_2]Cl$ is found to be the most active DNA cleaver, in agreement with a better stability of BDPEA in oxidizing conditions.

Keywords Polypyridine ligand · Manganese complexes · Iron complexes · Copper complexes · Oxidative DNA cleavage

Abbreviations *BDPEA:* bis[di-1,1-(2-pyridyl) ethyl]amine · *BDPMA*: bis[di(2-pyridyl)methyl]amine *MTBE*: methyl *tert*-butyl ether · *TPIP*: 1,3,3-tris (2-pyridyl)-3*H*-imidazo[1,5-*a*]pyridin-4-ium

Supplementary material Figures S1–S9 containing additional supporting data are available in electronic form on Springer Verlag's server at http://dx.doi.org/10.1007/s007750000177

C. Hemmert · M. Pitié · M. Renz · H. Gornitzka · S. Soulet
B. Meunier (✉)
Laboratoire de Chimie de Coordination du CNRS,
205 route de Narbonne, 31077 Toulouse cedex 4, France
E-mail: bmeunier@lcc-toulouse.fr
Fax: + 33-5-61553003

Introduction

Oxidative DNA cleavage is a fascinating area which includes studies on the mechanism of action of activated iron-bleomycin, an efficient anticancer drug [1, 2, 3, 4], iron-EDTA derivatives [5], copper-phenanthroline complexes [6], nickel compounds [7] and metalloporphyrins [8]. The driving force of this research field is the development of biological tools to study DNA structures, the preparation of new DNA footprinting agent, the study of the DNA oxidations or the elaboration of potential antitumoral or antiviral agents [4, 9]. In parallel to the development of oxidative DNA cleavers, non-redox-active metal complexes have also been used to accelerate the hydrolysis of the phosphodiester backbone of RNA and DNA [10, 11, 12, 13].

Owing to the fact that all these complexes show their own selectivity for a cleavage mechanism or for DNA interaction, the design of new DNA cleavage agents is of great interest. A wide range of metal complexes involving nitrogen ligands, based on macrocycles or Schiff bases or containing pyridine, pyrimidine or imidazole groups, have been used for DNA cleavage (see [14, 15, 16, 17] for some recent papers). In particular, polypyridine ligands have been used in order to prepare bleomycin analogues [15]. Their iron complexes realized efficient DNA cleavage at submicromolar concentration in the presence of reductant or hydrogen peroxide.

We have recently prepared tetrapyridyl ligands and corresponding first-row transition metal complexes, in order to investigate their capacities as biomimetic catalysts. The first generation of these ligands was the bis [di(2-pyridyl)methyl]amine (BDPMA) ligand (Fig. 1), which has been synthesized in a one-pot two-step

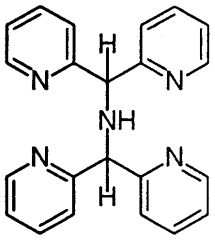

BDPMA

Fig. 1 Representation of BDPMA

reaction from di(2-pyridyl)methylamine and di(2-pyridyl) ketone on a large scale and with a good yield (70%) [18].

The catalytic activity of the corresponding mononuclear iron(III) complex, $[Fe(BDPMA)](NO_3)_3$, was tested in the oxidation of pollutants [19]. This complex is able to catalyze the oxidative degradation of polychlorophenols in the presence of potassium monopersulfate as oxidant to quinones, but the catalyst was degraded after a few catalytic cycles (between 22 and 27 cycles) [19].

The oxidative activity, the water solubility of the complex and its cationic charge (which allows electrostatic interactions with the negatively charged DNA) make $[Fe(BDPMA)](NO_3)_3$ a suitable candidate to conduct oxidative DNA degradation studies. Moreover, to avoid the fragility of BDPMA, we have prepared a second generation of tetrapyridine ligands, namely bis[di-1,1-(2-pyridyl)ethyl]amine (BDPEA) (Scheme 1), where the two hydrogen atoms of the benzylic positions α to the heteroatom were replaced by methyl groups.

Since the redox properties, and consequently the DNA cleavage activity, can be modulated by the nature of the metal complexed to the ligand, three well-known active metals have been complexed to BDPMA and BDPEA: iron(III), copper(II) and manganese(II). The preparation, characterization and X-ray structures of the three corresponding mononuclear complexes, $Mn(BDPEA)Cl_2$ (**1**), $[Fe(BDPEA)Cl_2]Cl$ (**2**) and [Cu(BDPEA)Cl]Cl (**3**), are presented. The nuclease activity of manganese(II), iron(III) and copper(II) complexes of both BDPMA and BDPEA ligands, when activated with ascorbate in the presence of dioxygen or hydrogen peroxide, are reported and compared. These metal complexes can be considered as good candidates for DNA cleavers based on the modeling of bleomycin.

Materials and methods

General

Commercially available reagents and all solvents were purchased from standard chemical suppliers and used without further purification. 1,3,3-Tris(2-pyridyl)-3*H*-imidazo[1,5-*a*]pyridin-4-ium (TPIP) was synthesized according to the literature procedure [20].

^1H and ^{13}C NMR spectra were recorded on a Bruker DPX 300 spectrometer with chloroform as internal reference. Elemental analyses were carried out by the "Service de Microanalyse du Laboratoire de Chimie de Coordination du CNRS". Mass spectrometry analyses were performed on a Nermag R1010 apparatus [FAB^+/*m*-nitrobenzyl alcohol (MNBA)] by the "Service de Spectrométrie de Masse de Chimie UPS-CNRS de Toulouse". UV-visible spectra were obtained on a Hewlett-Packard 8452A diode array spectrophotometer, using cuvettes of 1 cm pathlength. EPR spectra were recorded on a Bruker ESP 300 in X-band, with an ER035M gaussmeter (NMR probe) and an EIP 548 hyperfrequencymeter. Magnetic susceptibilities were determined by the Faraday method at room temperature, with a $HgCo(SCN)_4$ matrix ($c/g=16.44\times10^{-6}$ emu cgs). The diamagnetism of the ligands was corrected using Pascal's constants. EPR and magnetism data were carried out by the "Service de Mesures Magnétiques du Laboratoire de Chimie de Coordination du CNRS".

Electrochemical measurements were carried out with an Electrokemat potentiostat, using the interrupt method to minimize the uncompensated resistance (IR) drop [21]. Electrochemical experiments were performed at room temperature in an airtight cell connected to a vacuum-argon line. The reference electrode consisted of a saturated calomel electrode (SCE) separated from the solution by a bridge compartment. The counter electrode was a spiral of ca. 1 cm^2 apparent surface area, made of Pt (8 cm long and 0.5 cm diameter). The working microelectrode was Au (250 μm diameter) for cyclic and linear voltammetry. For electrolysis experiments, an Au spiral of ca. 1 cm^2 apparent surface area (10 cm long and 0.5 cm diameter) was used. The supporting electrolyte was Bu_4NPF_6 and the solvent used was MeCN. All solutions measured were 1.2–1.5 mM in complex and 0.1 M in supporting electrolyte.

Preparation of bis[di-1,1-(2-pyridyl)ethyl]amine)]

Under vigorous stirring and a nitrogen atmosphere, 1 mL of a 3 M solution of MeMgI in Et_2O was added dropwise to a solution of 300 mg (7.49×10^{-4} mol) of TPIP in 20 mL of dry toluene. After 2 h, 2 mL of a saturated NH_4Cl solution was added and the solvent evaporated. The residue was dissolved in 10 mL CH_2Cl_2 and washed with 10 mL of a 2 M NaOH solution. After drying with $MgSO_4$, the solvent was evaporated, the residue dissolved in 1 mL CH_2Cl_2 and exposed to a pentane atmosphere overnight. A yield of 209 mg (73%) of BDPEA was obtained as colorless crystals. ^1H NMR (300 MHz, $CDCl_3$, 25 °C): δ=1.48 (s, 6H), 5.96 (brs, 1H, N-H), 7.08 (ddd, *J*=1.7, 4.8, 6.6 Hz, 4H, 2-H), 7.56 (dt, *J*=1.8, 8.1 Hz, 4H, 3-H), 7.61 (ddd, *J*=1.1, 1.7, 8.1 Hz, 4H, 4-H), 8.55 (ddd, *J*=1.1, 1.7, 4.8 Hz, 4H, 1-H). ^{13}C NMR (75 MHz, $CDCl_3$, 25 °C): δ=26.3 (q, C-7), 65.6 (s, C-6), 121.5 (d, C-2), 122.3 (d, C-4), 136.4 (d, C-3), 148.5 (d, C-1), 168.7 (s, C-5). $C_{24}H_{23}N_5 0.4C_5H_{12} 0.5H_2O$ (419.35): calcd. C 74.46, H 6.92, N 16.70; found C 74.58, H 6.55, N 16.70. MS (FAB), *m/z* (%): 382 (57) [*M*+1], 303 (16) [*M*–py], 183 (100) [di(2-pyridyl)ethyl].

Preparation of dichloro[bis[di-1,1-(2-pyridyl)ethyl]amine)] manganese(II), $Mn(BDPEA)Cl_2$ (**1**)

BDPEA (21 mg, 5.5×10^{-5} mol) and $MnCl_2{\cdot}4H_2O$ (11 mg, 5.5×10^{-5} mol) were dissolved separately in a total volume of 2 mL of MeOH and then mixed. The resulting solution was stirred for 15 min and than allowed to stand in a methyl *tert*-butyl ether (MTBE) bath for 3 days. After washing with MTBE and drying under vacuum, 20 mg (72%) of pale yellow crystals of **1** were obtained. $C_{24}H_{23}Cl_2MnN_5{\cdot}3H_2O$ (561.36): calcd. C 51.35, H 5.21, N 12.48; found C 51.56, H 5.16, N 12.36. FAB-MS, *m/z* (%): 471 (100) $[M–Cl]^+$. UV/Vis (MeOH): λ_{max} (ε M^{-1} cm^{-1}) =208 nm (23,300), 260 (17,500).

Dichloro[bis[di-1,1-(2-pyridyl)ethyl]amine)]iron(III) chloride, [Fe(BDPEA)Cl_2]Cl (**2**)

BDPEA (50 mg, 1.31×10^{-4} mol) and $FeCl_3$ (21 mg, 1.31×10^{-4} mol) were dissolved separately in a total volume of 2 mL of MeOH and mixed together. The resulting solution was stirred for 15 min and than allowed to stand in a MTBE bath for 2 days. After washing with MTBE and drying under vacuum, 44 mg (56%) of orange crystals **2** were obtained. $C_{24}H_{23}Cl_3FeN_5{\cdot}3MeOH{\cdot}3H_2O$ (693.86): calcd. C 46.74, H 5.96, N 10.09; found C 46.56, H 5.85, N 10.14. MS (FAB), *m/z* (%): 507 (1.6) $[M–Cl]^+$, 472 (100) $[Fe^{II}(BDPEA)Cl]^+$. UV/Vis (MeOH): λ_{max} (ε M^{-1} cm^{-1})=210 nm (57,200), 258 (42,300), 344 (8000).

Chloro[bis[di-1,1-(2-pyridyl)ethyl]amine)]copper(II) chloride, [Cu(BDPEA)Cl]Cl (**3**)

BDPEA (83 mg, 2.18×10^{-4} mol) and $CuCl_2$ (29 mg, 2.18×10^{-4} mol) were dissolved separately in a mixture of MeCN/MeOH (1:1, total volume 3 mL) and then mixed. The resulting solution was stirred for 15 min and than allowed to stand in a MTBE bath for 1 day. After washing with MTBE and drying under vacuum, 85 mg (76%) of ultramarine blue crystals of **3** were obtained. $C_{24}H_{23}Cl_2CuN_5$ (515.93): calcd. C 55.87, H 4.49, N 13.58; found C 55.64, H 4.36, N 13.43. FAB-MS, *m/z*: (%) 479 (100) $[M–Cl]^+$, 444 (4.6) $[Cu^I(BDPEA)]^+$, 183 (7.6) [di(2-pyridyl)ethyl]. UV/Vis (MeOH): λ_{max} (ε M^{-1} cm^{-1})=208 nm (19,400), 258 (14,100), 720 (106).

Crystallography

Crystal data for BDPEA and complexes **1**–**3** are presented in Table 1 . All data were collected at low temperatures using an oil-coated shock-cooled crystal [22] on a Stoe-IPDS diffractometer with Mo Kα (λ=0.71073 Å) radiation. The structures were solved by direct methods using SHELXS-97 [23] and refined with all data on F^2 using SHELXL-97 [24]. All non-hydrogen atoms were refined anisotropically. The hydrogen atoms of the molecules were geometrically idealized and refined using a riding model. Selected bond lengths of complexes **1**–**3** can be found in Table 2 . Crystallographic data (excluding structure factors) for the structures reported in this paper have been deposited with the Cambridge Crystallographic Data Centre as supplementary publication no. CCDC-112641 for BDPEA, CCDC-141423 for **1**, CCDC-141424 for **2** and CCDC-141425 for **3**. Copies of the data can be obtained free of charge on application to CCDC, 12 Union Road, Cambridge CB2 1EZ, UK (e-mail: deposit@ccdc.cam.ac.uk, Fax: +44-1223-336033).

DNA cleavage experiments

Stock solutions of metal salts (10 mM in water) and ligands (5 mM in DMF) were prepared just before use. Metallations by $MnCl_2{\cdot}4H_2O$, $FeCl_3$ or $CuCl_2$ of BDPMA [25, 26] and BDPEA were performed by using 1 equivalent of desired ligand and metal salt in a DMF/water mixture (2:8 v/v, the final concentration being 1 mM) during 4 h at room temperature before dilution of the corresponding complex with water. To 10 µL of ΦX174 supercoiled DNA (7 nM, 40 µM in bp) in 20 mM Tris-HCl buffer (pH 7.2) was added 5 µL of the desired complex (4 or 0.4 µM). After 30 min at room temperature, DNA cleavage was initiated by addition of an aqueous solution of L(+)-ascorbic acid sodium salt (ascorb, 5 µL, 0.4 mM) or of H_2O_2 (5 µL, 4 mM), and samples were incubated 1 h at 37 °C under aerobic conditions. Consequently, in the final volume of 20 µL, the concentrations of DNA, complex, ascorbate and hydrogen peroxide are 3.5 nM, 1 or 0.1 µM, 0.1 mM and 1 mM, respectively. A 7.5 µL portion of a solution of 75% (v/v) glycerol/TBE buffer and 0.05% bromophenol blue (w/v) was then added, and then the samples were immediately loaded on agarose gel (0.8%) containing 1 µg/mL of ethidium bromide (TBE buffer=90 mM Tris/90 mM boric acid/3 mM EDTA). Electrophoresis was run at constant current (25 mA for 15 h) in a TBE buffer in the

Table 1 Crystal structure data for BDPEA and complexes **1**–**3**

	BDPEA	**1**	**2**	**3**
Formula	$C_{26.5}H_{29}N_5$	$C_{24}H_{23}Cl_2MnN_5$	$C_{26}H_{31}Cl_3FeN_5O_2$	$C_{24}H_{23}Cl_2CuN_5$
M_r	417.55	507.31	607.76	515.91
Temperature (K)	173(2)	173(2)	173(2)	173(2)
Crystal system	Triclinic	Triclinic	Orthorhombic	Monoclinic
Space group	$P\bar{1}$	$P\bar{1}$	$Pna2_1$	$P2_1/n$
a (Å)	8.483(1)	9.198(1)	18.534(3)	8.614(1)
b (Å)	10.821(2)	9.401(1)	12.730(2)	16.791(2)
c (Å)	14.621(2)	15.211(2)	11.794(3)	16.206(2)
α (°)	68.30(2)	97.99(2)	90	90
β (°)	85.78(2)	97.09(2)	90	96.93(2)
γ (°)	68.46(2)	111.83(2)	90	90
V (Å^3)	1156.9(3)	1187.0(2)	2782.7(9)	2326.9(5)
Z	2	2	4	4
$\rho_{(calc)}$ [Mg m^{-3}]	1.199	1.419	1.451	1.473
F(000)	446	522	1260	1060
Cryst. size (mm)	0.5, 0.3, 0.3	0.4, 0.3, 0.1	0.4, 0.4, 0.1	0.7, 0.6, 0.1
$2\theta_{max}$ (°)	47	47	44	47
Reflections collected	9351	8813	17,988	18,797
Independant reflections	3249	3237	3293	3411
Absorption correction	None	None	None	Numerical
T_{min}, T_{max}	–	–	–	0.7609/0.8756
Parameters	358	294	343	341
R ($I>2\sigma(I)$)	0.0413	0.0430	0.0563	0.0270
wR2[a] (all data)	0.1060	0.1025	0.1049	0.0541
$(\Delta/\rho)_{min}$ (e Å^{-3})	–0.159	–0.342	–0.418	–0.297
$(\Delta/\rho)_{max}$ (e Å^{-3})	0.147	0.511	0.449	0.236

[a] $wR2=\{[\Sigma w(F_c^2-F_o^2)^2]/[\Sigma w(F_o^2)^2]\}^{1/2}$

Table 2 Selected bond lengths (Å) for $Mn(BDPEA)Cl_2$ (**1**), $[Fe(BDPEA)Cl_2]Cl$ (**2**) and [Cu(BDPEA)Cl]Cl (**3**)

Mn-N(1)	2.276(4)	Mn-N(5)	2.258(3)
Mn-N(2)	2.251(4)	Mn-Cl(1)	2.384(1)
Mn-N(4)	2.345(3)	Mn-Cl(2)	2.493(1)
Fe-N(1)	2.195(9)	Fe-N(5)	2.191(13)
Fe-N(2)	2.039(12)	Fe-Cl(1)	2.257(4)
Fe-N(4)	2.076(11)	Fe-Cl(2)	2.272(4)
Cu-N(1)	1.993(2)	Cu-N(5)	2.013(2)
Cu-N(2)	1.978(2)	Cu-Cl(1)	2.216(1)
Cu-N(4)	2.240(3)		

dark, in order to avoid any possible photoreactions (control experiments run in the presence of complexes and activating agents confirmed that ethidium bromide was unable to generate photocleavage). Bands were located by UV light (254 nm), photographed and quantified by densitometry (Hoefer GS-300) on the negatives. The correction coefficient 1.47 was used for decreased stainability of form I DNA versus forms II and III [27]. When only DNA forms I and II were formed, the average number of single-strand scissions per DNA molecule, expressed as *S*, was considered to be equal to –ln(fraction of form I) according to a Poisson distribution. When DNA form III is present, *S* was calculated from the following equation: % form I+% form II=$[1\text{-}S(2h+1)/2L]^{S/2}$, where *h* is the distance between nicks on opposite strands needed to produce a linear molecule (16 bp) and *L* is the total number of bps in *Φ*X174 (5386) [28].

Results and discussion

Ligand synthesis and preparation of complexes

We recently investigated the synthesis and the chemical behavior of manganese(II), iron(III), cobalt(II) and copper(II) complexes of BDPMA. The determination of the crystal structures of these complexes allowed us to understand the versatility of this tetrapyridyl ligand in the presence of certain metallic salts, owing to the presence of fragile benzylic C-H bonds to the central heteroatom [20, 25]. Two different classes of compounds have been crystallographically characterized with this ligand. Complexes containing the intact BDPMA ligand, like $Mn(BDPMA)Cl_2$ [25], $[Fe_2(BDPMA)_2(O)Cl_2]Cl_2$ [25] and $Cu(BDPMA)Cl_2$ [26], constituted the first category. The second one corresponded to an oxidative degradation product of the starting BDPMA ligand, namely the cationic species TPIP [20, 25]. During different attempts to use TPIP as a potential ligand, we have been able to isolate complexes containing a new ligand, namely [di(2-pyridyl)methoxymethyl][di(2-pyridyl)]imine, and involving a modification (probably metal-assisted) of the starting TPIP ligand, by nucleophilic attack of a methanol molecule and opening of the imidazolium ring [25, 26]. Taking into account the reactivity of TPIP, we have successfully used this ligand to prepare a more robust tetrapyridyl ligand. The synthesis of BDPEA was carried out from TPIP with a methyl Grignard reagent (Scheme 1).

By addition of one equivalent of MeMgI, the imidazolium ring was opened and the intermediate imine **1** was formed as a neutral molecule (Scheme 1). This latter compound is also an electrophile which reacts quickly with a second equivalent of the Grignard reagent. In fact, the TPIP cation could be considered as a masked di-imine. The BDPEA ligand was crystallized by slow evaporation of a methanolic solution in a pentane atmosphere with a good yield (73%), giving colorless crystals suitable for X-ray analysis (Fig. 2).

By mixing stoichiometric amounts of BDPEA and $MnCl_2{\cdot}4H_2O$, $FeCl_3$ or $CuCl_2$ in methanol solution, and allowing the resulting mixture to stand in a MTBE bath (for 1–3 days), the three corresponding complexes $Mn(BDPEA)Cl_2$ (**1**), $[Fe(BDPEA)Cl_2]Cl$ (**2**) and [Cu(BDPEA)Cl]Cl (**3**) were crystallized respectively, with reasonable yields (56–76%).

X-ray crystal structures and characterization of $[Mn(BDPEA)Cl_2]$, $[Fe(BDPEA)Cl_2]Cl$ and [Cu(BDPEA)Cl]Cl

The X-ray structures of $[Mn(BDPEA)Cl_2]$ (**1**), $[Fe(BDPEA)Cl_2]Cl$ (**2**) and [Cu(BDPEA)Cl]Cl (**3**) are depicted in Fig. 3 and selected bond lengths and angles are listed in Table 2 .

Complexes **1**–**3** consisted of mononuclear entities, neutral for $[Mn^{II}(BDPEA)Cl_2]$ and monocationic for $[Fe^{III}(BDPEA)Cl_2]^+$ and $[Cu^{II}(BDPEA)Cl]^+$. In all three complexes, BDPEA acts as a tetradentate ligand

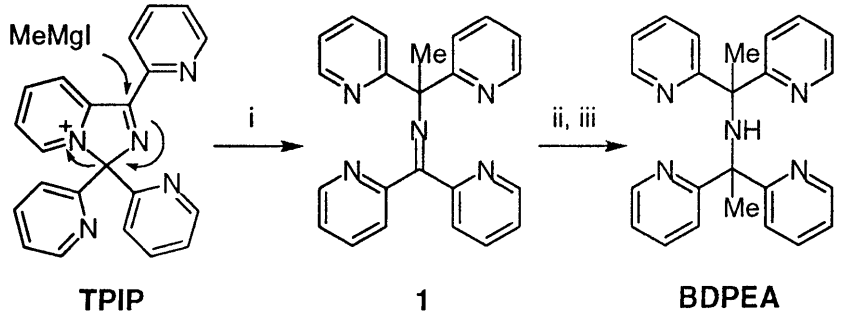

(i) MeMgI. (ii) MeMgI. (iii) H_2O, H^+.

Scheme 1 Synthesis of BDPEA from TPIP

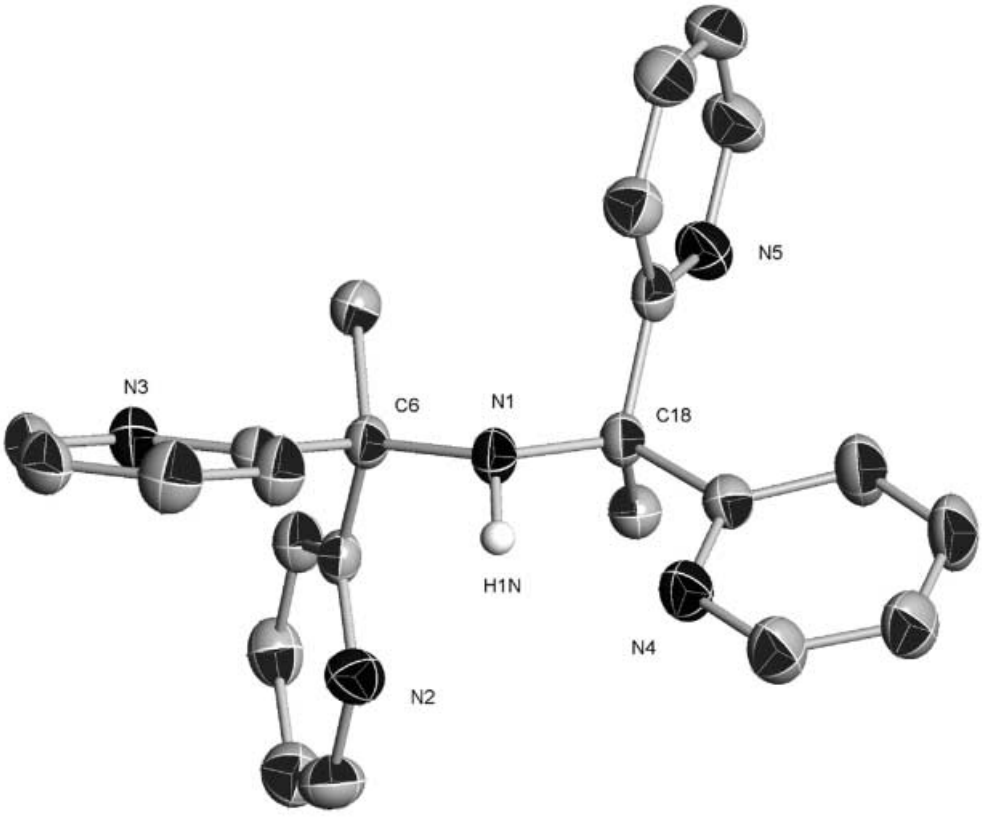

Fig. 2 Crystal structure of BDPEA. Non-discussed hydrogen atoms are omitted for clarity. Anisotropic displacement parameters are depicted at a probability level of 50%. A non-coordinated molecule of pentane and methyl and pyridine hydrogen atoms are omitted for clarity. N1-C6 1.472(2) Å; N1-C18 1.475(2) Å

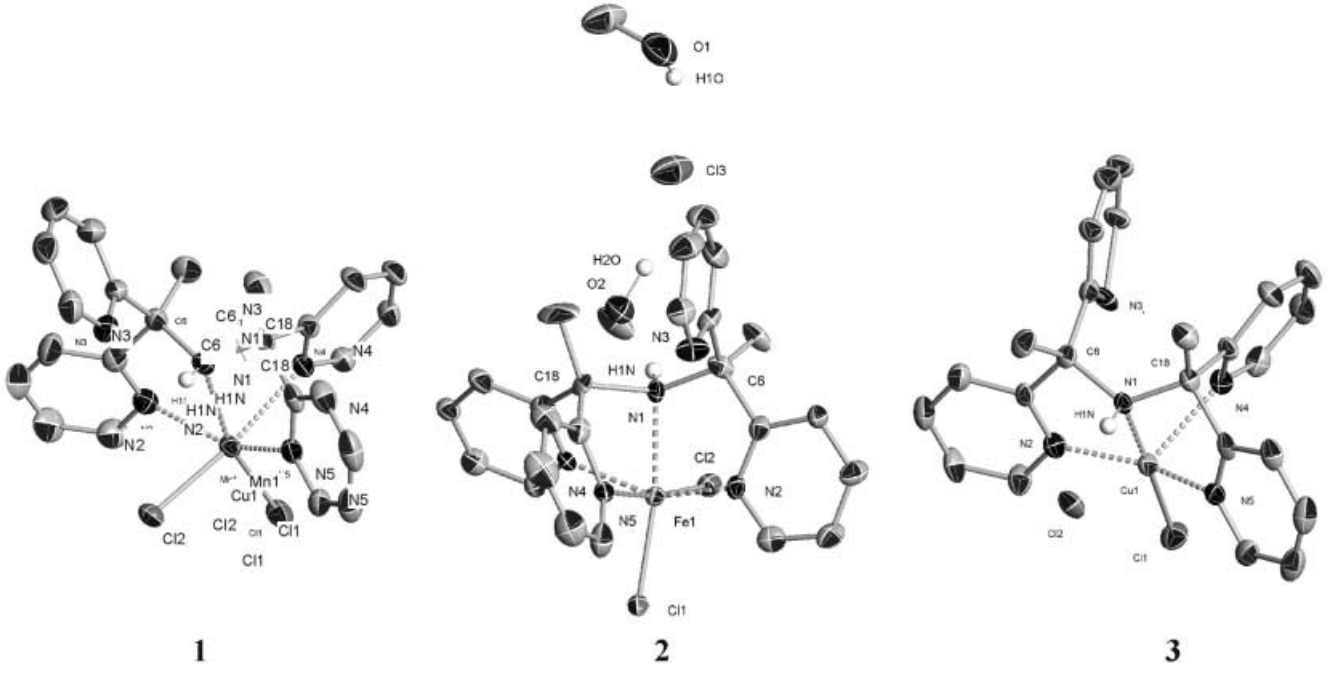

Fig. 3 Crystal structures of $Mn(BDPEA)Cl_2$ (**1**), $[Fe(BDPEA)Cl_2]Cl$ (**2**) and [Cu(BDPEA)Cl]Cl (**3**). Non-discussed hydrogen atoms are omitted for clarity

and is coordinated to the metal center by the secondary amine nitrogen and three pyridine nitrogen atoms, the fourth pyridine remaining uncoordinated. The most important difference between the free and coordinated BDPEA ligand is the elongation of the central N-C distances (N1-C6 and N1-C18), owing to the steric constraints involved by complexation [N1-C6 1.472(2) Å for BDPEA, 1.487(5) Å for **1**, 1.569(15) Å for **2** and 1.510(4) Å for **3**; N1-C18 1.475(2) Å for BDPEA, 1.493(5) Å for **1**, 1.656(15) Å for **2** and 1.494(4) Å for **3**; see Supplementary material]. It is interesting to note that the N_{amine}-C bond lengths are quite identical in the free ligand while this is not the case in complexes **1**–**3**, the most elongated one being on the side where two pyridines are coordinated.

The geometrical environments of the metal ions in **1** and **2** are best described as distorted octahedral. In **1**, the equatorial plane is formed by two pyridine nitrogens, arising from each di(2-pyridyl)ethyl moiety, the secondary amine nitrogen and one chloride ion.

The equatorial Mn-N bond lengths are typical, ranging from 2.258(3) to 2.276(4) Å. The axial positions are occupied by one pyridine nitrogen and a second chloride ion [Mn-N4 2.345(3) and Mn-Cl2 2.493 (1) Å]. Exactly the same arrangement was obtained with the BDPMA ligand in the corresponding mononuclear manganese(II) complex [25]. One interesting feature in **1** is the presence of an intramolecular hydrogen bond between H(1N) and N3 with a bond length of 2.29(5) Å [distance N1···N3 2.706(5) Å].

In contrast to **1**, the equatorial plane of complex **2** includes three pyridine nitrogen atoms of BDPEA, with a mean distance of 2.102(12) Å, while the secondary amine nitrogen atom is located in an axial position, with a longer distance [Fe-N1 2.195(9) Å]. The coordination sphere is completed by two chloride ions. The electroneutrality of complex **2** is ensured by a third ionic chloride. Cl3 is caught between two methanol molecules and thus stabilized through a hydrogen bond lattice, with bond lengths of 2.18(6) and 2.17(7) Å for H(2O)···Cl3 and H(1O)···Cl3, respectively [distances O2···Cl3 3.108(10) and O1···Cl3 3.067(10) Å]. An interaction of 1.97 Å between H(1N) and O2 propagated this lattice up to the cationic complex **2** [distance N1···O2 3.067(10) Å]. For comparison, the analogous complex with BDPMA was crystallized as a (μ-oxo)diiron(III) core of general formula $[Fe_2(BDPMA)_2(O)Cl_2]Cl_2(MeOH)_2$; each iron ion is in an approximate octahedral geometry and coordinated to four nitrogen atoms of BDPMA, the bridging oxygen atom and a chloride anion [25].

The crystal structure of **3** contains a CuN_4Cl entity in a slightly distorted square pyramidal geometry. The basal plane is identical as that in complex **1** and the N4 pyridine nitrogen occupies the axial position, with a bond length of 2.240(3) Å.

The three equatorial Cu-N distances lie in the range 1.978(2)–2.013(2) Å, which are usual values. The L_{ax}-Cu-N_{eq} angles vary from 80.37(10)° for N1-Cu-N5 to 98.67(7)° for N5-Cu-Cl1 (see Supplementary material), all being within 10° of the ideal 90°. Once again, the hydrogen on the secondary amine affords a stabilization of the second non-coordinated chloride, through a H(1N)···Cl2 interaction of 2.36(3) Å [distance of N1···Cl2 3.143(3) Å]. The corresponding mononuclear copper(II) complex of BDPMA displayed a distorted trigonal bipyramidal geometry, involving only three nitrogen atoms of BDPMA (coming from the secondary amine and two pyridine groups, respectively) and two chloride anions [26].

Properties of complexes **1**–**3**

The X-band EPR spectrum of $Mn(BDPEA)Cl_2$ (**1**), in a 80:20 CH_2Cl_2/DMF glass at 95 K, exhibits several fine-structure resonances spread out over 4000 G. One strong signal centered at g=2.01 splits into the characteristic ^{55}Mn six-line pattern. The hyperfine coupling constant A of 92 G is consistent with a Mn(II) in a octahedral environment with nitrogen ligands. In the 1200–2200 G region, at least two resonances are superimposed, one of them being split into an 11-line pattern with a hyperfine coupling constant of 40 G, probably indicating the presence of a dimeric species in frozen solution. A Faraday balance measurement at room temperature on a crystalline sample gives an effective magnetic moment per mononuclear complex of 5.99 μB, which is consistent with a high-spin Mn(II) species. At 95 K, the X-band EPR spectra of a crystalline sample and a glass (in a 80:20 mixture of CH_2Cl_2/DMF plus a drop of MeOH) of $[Fe(BDPEA)Cl_2]Cl$ (**2**) both exhibit one resonance centered at g=4.34 and 4.37, respectively, which is typical of a rhombically distorted high-spin iron(III) species. A Faraday balance measurement at room temperature on a crystalline sample give an effective magnetic moment per mononuclear complex of 5.88 μB, which is consistent with the EPR measurements. At 95 K, the X-band EPR spectrum of a crystalline sample of [Cu(BDPEA)Cl]Cl (**3**) is best described as an isotropic signal centered at 2.08. The EPR spectrum of complex **3**, in an 80:20 mixture of CH_2Cl_2/DMF glass at 95 K, is resolved into parallel and perpendicular components. It exhibits two identifiable magnetic g values along with the corresponding copper (I=3/2) hyperfine splitting constants, with the following values: $g_{\|}$=2.23, $A_{\|}$=166 G and $g_{\perp}$=2.04. Additional very weak signals are discernable on the $g_{\perp}$ component.

Electrochemical measurements of all complexes were carried out in MeCN with tetrabutylammonium hexafluorophosphate as supporting electrolyte (Bu_4NPF_6). Results are summarized in Table 3. Surprisingly, none of the manganese(II) complexes are electroactive in the potential range of –1500 to 1500 mV. Cyclic voltammograms of both iron(III) complexes show a one-electron (confirmed by bulk

Table 3 Electrochemical measurements of $[Fe_2(BDPMA)_2OCl_2]Cl_2$, $Cu(BDPMA)Cl_2$ and complexes **2** and **3**

	Cyclic voltammetry[a]			Linear voltammetry[b]
	Ep_c (mV/ECS)	Ep_a (mV/ECS)	Ip_c/Ip_a	$E_{1/2}$ (mV/ECS)
$[Fe_2(BDPMA)_2OCl_2]Cl_2$	182	255	1.00	200
$[Fe(BDPEA)Cl_2]Cl$ (**2**)	144	238	0.97	200
$Cu(BDPMA)Cl_2$	–275	–139	0.56	–276
[Cu(BDPEA)Cl]Cl (**3**)	–374	–246	0.78	–301

[a]Scan rate 100 mV s–1
[b]Scan rate 5 mV s^{-1}

electrolysis) quasi-reversible [peak to peak separation ΔE_p=73 mV for $[Fe_2(BDPMA)_2(O)Cl_2]Cl_2$ and 93 mV for **2**] electrochemical reduction close to 200 mV/ECS. The ip_c/ip_a ratios of ca. 1 for both complexes are indicative of a good chemical stability of the reduced species and this was confirmed by the cyclic voltammogram measured after coulometry (the Ep_c and Ep_a values are identical to those before electrolysis). The electrochemical behavior of the copper complexes is characterized by quasi-reversible [ΔEp=136 for $Cu(BDPMA)Cl_2$ and 128 for **3**] one-electron (confirmed by bulk electrolysis) reductions, with $E_{1/2}$ values close to –280 to –300 mV/ECS. For $Cu(BDPMA)Cl_2$, the ip_c/ip_a ratio of 0.56 is indicative of a poor chemical stability of the reduced species. This fact was indeed confirmed for both complexes after electrolysis: the cyclic voltammograms are totally different, the UV-visible spectra show no characteristic Cu(I) MLCT and no EPR signal indicative of the presence of a radical on the ligand (g=2.00) could be detected. So the metal-centered reduction processes lead probably to copper(I) complexes, which undergo further chemical reactions. This could be explained by the involvement of structural changes too dramatic to stabilize a tetrahedral geometry around a copper(I) cation.

For all complexes, an intense anodic peak appears between 1100 and 1300 mV/ECS, which can be attributed to the oxidation of the chloride anions. Although the experimental conditions are different from those of DNA cleavage experiments, the electrochemical results are in a good agreement with the DNA cleavage activity observed for the different complexes (see discussion below).

DNA cleavage activity of complexes

The DNA cleavage activities of $FeCl_3$, $CuCl_2$ or $MnCl_2$ complexes of BDPMA and BDPEA have been compared. The relaxation of supercoiled circular ΦX174 DNA (form I) into relaxed (form II) and linear (form III) conformations was used to quantify the relative DNA cleavage activity of the different complexes. All complexes have been tested at 1 μM concentration in order to have a direct comparison. We chose to test two modes of activation generally used with ferric complexes of bleomycin in DNA cleavage experiments: a reducing agent (ascorbate) in the presence of air or an oxidant, hydrogen peroxide. This choice of activation modes has been based on preliminary attempts with the BDPMA·$FeCl_3$ complex, which showed that dithiothreitol can also be used as reductant and $KHSO_5$ as oxidant. H_2O_2 or ascorbate in the presence of air should be able to activate the presently studied iron complexes (as observed for other iron complexes used as DNA cleavers) [1, 6, 15, 16], but also copper or manganese complexes since they have been previously used successfully for cupric complexes of phenanthroline derivatives [6, 17, 29, 30] or different manganese complexes [31, 32, 33]. We also checked that control experiments with $FeCl_3$, $CuCl_2$ or $MnCl_2$ without ligand (or ligand without metal), in the presence or absence of ascorbate or H_2O_2, did not show any DNA breaks at the concentrations used in the present study. Table 4 summarizes the results obtained.

When metallations were conducted in the presence of $MnCl_2$, Mn^{II} complexes of BDPMA or BDPEA were inactive [similar results have been obtained by metallation of BDPMA by $Mn^{III}(OAc)_3$]. In the case of $CuCl_2$ complexes, only a low DNA cleavage efficiency was observed with the two modes of activation, but the ferric complexes were significantly more active. In the presence of 1 μM of BDPEA·$FeCl_3$ or BDPMA·$FeCl_3$ complex, ΦX174 supercoiled DNA was cleaved in form II and form III DNA when activation was performed with ascorbate. The comparison of cleavage pattern with experiments conducted with only 0.1 μM of iron complexes showed that the amount of DNA breaks increased as a function of the iron complex concentration, since form I was only transformed in form II at this concentration. The fact that only form II was observed for 0.1 μM of complexes suggested: (1) a progressive transformation of ΦX174 form I to form II and then to form III according to an activated species carrying out single-strand DNA cleavage (which transformed form I in form II); (2) a poor or an absence of DNA sequence selectivity (which might generate additional single strand breaks in the vicinity of the initial DNA cleavage sites leading to form III before the total diseapparance of form I). These results led us to tentatively quantify the amount of single-strand cleavage (S) as in [23]. The

Table 4 DNA cleavage activity of the iron, manganese and copper complexes of BDPMA or BDPEA tetrapyridyl ligands using supercoiled DNA. *S* corresponds to the average number of single-strand breaks per DNA molecule

	% Form I	% Form II	% Form III	*S*
Control DNA	75±5	25±5	0	0.25±0.05
BDPMA·$FeCl_3$ (1 μM)/ascorb/O_2	0	90±5	10±5	8±2
BDPMA·$FeCl_3$ (0.1 μM)/ascorb/O_2	35±5	65±5	0	1.0±0.1
BDPEA·$FeCl_3$ (1 μM)/ascorb/O_2	0	70±10	30±10	15±3
BDPEA·$FeCl_3$ (0.1 μM)/ascorb/O_2	10±5	90±5	0	2.3±0.3
BDPMA·$CuCl_2$ (1 μM)/ascorb/O_2	60±5	40±5	0	0.51±0.05
BDPEA·$CuCl_2$ (1 μM)/ascorb/O_2	60±5	40±5	0	0.51±0.05
BDPMA·$MnCl_2$ (1 μM)/ascorb/O_2	75±5	25±5	0	0.25±0.05
BDPEA·$MnCl_2$ (1 μM)/H_2O_2	80±5	20±5	0	0.22±0.05
BDPMA·$FeCl_3$ (1 μM)/H_2O_2	25±5	75±5	0	1.4±0.2
BDPMA·$FeCl_3$ (0.1 μM)/H_2O_2	60±5	40±5	0	0.51±0.05
BDPEA·$FeCl_3$ (1 μM)/H_2O_2	0	50±10	40±10	18±3
BDPEA·$FeCl_3$ (0.1 μM)/H_2O_2	30±5	70±5	0	1.2±0.2
BDPMA·$CuCl_2$ (1 μM)/H_2O_2	50±5	50±5	0	0.7±0.1
BDPEA·$CuCl_2$ (1 μM)/H_2O_2	80±5	20±5	0	0.22±0.05
BDPMA·$MnCl_2$ (1 μM)/H_2O_2	80±5	20±5	0	0.22±0.05
BDPEA·$MnCl_2$ (1 μM)/H_2O_2	80±5	20±5	0	0.22±0.05

cleavage pattern and the quantification showed clearly that BDPEA·$FeCl_3$ was a better nuclease than BDPMA·$FeCl_3$ in an attempt for a more stable complex (in the case of ascorbate activation, *S*=15 and 2.3, for respectively 1 and 0.1 μM in complex, for BDPEA·$FeCl_3$, versus 8 and 1.0 for BDPEA·$FeCl_3$).

Iron complexes could be also activated with H_2O_2 and also in this case BDPEA·$FeCl_3$ was the more active (*S*=18 and 1.2 for 1 and 0.1 μM, respectively, versus 1.4 and 0.51 in the case of BDPMA·$FeCl_3$). These results should indicate that the ferric complexes could be activated into a Fe^{III}-OOH form (as precedented by the intermediate proposed for the iron complex of bleomycin or other polypyrimidines) ([1, 15, 34, 35] and references therein) or a Fe^{IV}=O species also proposed in the case of the oxidation of chlorinated phenols by a (BDPMA)Fe^{III} complex activated by $KHSO_5$ [19]. These activated forms could be also involved in the case of ascorbate activation in the presence of air [the one-electron reduction of dioxygen to superoxide anion, followed by dismutation of this latter species, can give hydrogen peroxide which can generate Fe(III)-OOH or Fe(IV)=O entities]. However, with BDPMA·$FeCl_3$ a higher DNA cleavage efficiency was observed in the case of ascorbate activation than for H_2O_2 activation (*S*=8 and 1.0 for ascorbate versus 1.4 and 0.51 for H_2O_2 for 1 and 0.1 μM of complex, respectively). So, it is reasonable to assume that several competitive oxidative species could be also formed during the activation of these iron complexes when using a reducing agent in the presence of air [6].

In order to obtain additional information regarding the mechanism of DNA cleavage, superoxide dismutase (SOD) or catalase were included in the investigation as potential inhibitors of the strand scission activity by BDPMA·$FeCl_3$ activated by ascorbate [28, 36]. A decrease of DNA cleavage up to 95% in the presence of SOD or catalase has been observed, in accordance with the formation of the active species proposed.

Conclusion

We described the synthesis and characterization of the novel robust polypyridyl ligand BDPEA and the corresponding mononuclear manganese(II), iron(III) and copper(II) complexes. The DNA cleavage activites of these complexes have been compared to those of Fe^{III}, Cu^{II} and Mn^{II} complexes of BDPMA (a less robust ligand unmethylated on the benzylic position). Iron(III) complexes of both BDPMA and BDPEA can be activated by ascorbate or H_2O_2 and create single-strand breaks on DNA at submicromolar concentration. The most active DNA cleaver is BDPEA·$FeCl_3$. However, the DNA affinity of these tetrapyridyl ligands has not been optimized. Since one of the pyridines is not involved in the coordination sphere of the corresponding complexes, this non-coordinating pyridine can be probably replaced with low effects on the chelation and redox properties of the ligand. Our next goal is to substitute this pyridine in order to increase the DNA affinity and to have the activated species in the closest possible vicinity to its DNA target in order to increase the DNA cleavage activity of these polypyridine complexes.

Acknowledgements We are grateful to the CNRS for financial support, especially to M.R. for a postdoctoral fellowship. The authors thank A. Mari and D. de Montauzon (LCC-CNRS) for magnetic and electrochemical measurements, respectively.

References

1. Burger RM (1998) Chem Rev 98:1153–1169
2. Hecht SM (1986) Acc Chem Res 19:383–391
3. Stubbe J, Kozarich JW (1987) Chem Rev 87:1107–1136
4. Pratviel G, Bernadou J, Meunier B (1998) Adv Inorg Chem 45:251–312
5. Dervan PB (1986) Science 232:464–471
6. Sigman DS, Mazumder A, Perrin DM (1993) Chem Rev 93:2295–2316
7. Burrows CJ, Rokita SE (1994) Acc Chem Res 27:295–301

8. Pitié M, Bernadou J, Meunier B (1995) J Am Chem Soc 117:2935–2936
9. Meunier B (ed) (1996) DNA and RNA cleavers and chemotherapy of cancer and viral diseases. Kluwer, Dordrecht
10. Williams NH, Takasaki B, Wall M, Chin J (1999) Acc Chem Res 32:485–493
11. Komiyama M, Takeda N, Shigekawa H (1999) Chem Commun 1443–1451
12. Williams NH, William C, Chin J (1998) J Am Chem Soc 120:8079–8087
13. Kimura E, Koike T (1997) Adv Inorg Chem 44:229–261
14. Guajardo RJ, Hudson SE, Brown SJ, Mascharak P (1993) J Am Chem Soc 115:7971–7977
15. Mialane P, Nivorojkine A, Pratviel G, Azéma L, Slany M, Godde F, Simaan A, Banse F, Kargar-Grisel T, Bouchoux G, Sainton J, Horner O, Guilhem J, Tchertanova L, Meunier B, Girerd JJ (1998) Inorg Chem 38:1085–1092
16. Silver GC, Trogler WC (1995) J Am Chem Soc 117:3983–3993
17. Pitié M, Meunier B (1998) Bioconjug Chem 604–611
18. Renz M, Hemmert C, Meunier B (1998) Eur J Org Chem 1271–1273
19. Hemmert C, Renz M, Meunier B (1999) J Mol Catal A 137:205–212
20. Renz M, Hemmert C, Donnadieu B, Meunier B (1998) Chem Commun 1635–1636
21. Cassoux P, Dartiguepeyron R, David C, de Montauzon D, Tommasino JB, Fabre PL (1994) Actual Chim 1:49–55
22. Stalke D (1998) Chem Soc Rev 27:171–178
23. Sheldrick GM (1990) Acta Crystallogr Sect A 46:467–473
24. Sheldrick GM (1997) Program for crystal structure refinement. Universität Göttingen
25. Hemmert C, Renz M, Gornitzka H, Soulet S, Meunier B (1999) Chem Eur J 5:1766–1774
26. Hemmert C, Renz M, Gornitzka H, Meunier B (1999) J Chem Soc Dalton Trans 3989–3994
27. Bernadou J, Pratviel G, Bennis F, Girardet M, Meunier B (1989) Biochemistry 28:7268–7275
28. Hertzberg RP, Dervan PB (1984) Biochemistry 23:3934–3945
29. Veal JM, Merchant K, Rill RL (1991) Nucleic Acids Res 19:3383–3388
30. Baudoin O, Teulade-Fichou MP, Vigneron JP, Lehn JM (1998) Chem Commun 2349–2350
31. Routier S, Joanny V, Zaparucha A, Vezin H, Catteau JP, Bernier JL, Bailly C (1998) J Chem Soc Perkin Trans 2 863–868
32. Burger RM, Freedman JH, Horwitz SB, Peisach J (1984) Inorg Chem 23:2217–2219
33. Griffin JH (1995) Bioorg Med Chem Lett 5:73–76
34. Sam JW, Tang XJ, Peisach J (1994) J Am Chem Soc 116:5250–5256
35. Westre TE, Loeb KE, Zaleski JM, Hedman B, Hogson KO, Solomon E (1995) J Am Chem Soc 117:1309–1313
36. Hertzberg RP, Dervan PB (1982) J Am Chem Soc 104:313–315